shows that in transition from the relaxed to the rigor state, the total amount of mass transfer is about twice as that found in Fig. 1 *c* and the loss of mass originates mostly from the region surrounding the backbone of thick filaments. On the other hand, with lowering of μ in the relaxed state (Fig. 1 *c*), loss of mass appears to be evenly distributed in areas surrounding both the thick and thin filaments. Furthermore, in Fig. 1 *b* the attachment of the rigor cross-bridges brings the gain of mass in such a way that the profile of the axially projected thin filament, with cross-bridges attached to it, appears enlarged by 5 nm in its apparent diameter. This behavior is in contrast to the case in Fig. 1 *c* where more relaxed cross-bridges become attached in the final state of lower ionic strength. In this case, there is also a gain of mass at the thin filament, but the apparent diameter is almost unchanged. Preliminary modeling shows that it is the increase in the apparent diameter of the thin filament profile and more severe loss of mass from the area surrounding the backbone that distinguish the rigor-relaxed difference map (Fig. 1 *b*) from the relaxed-relaxed difference map (Fig. 1 *c*). One possible explanation could be that in the relaxed state only a small part of the myosin head is immobilized by attachment and the rest of the head may move around the thin filament freely. This type of attachment could create a rather disordered array of cross-bridges. From an end-on view, at the present spatial resolution, attached cross-bridges would appear hardly different from the detached ones. Therefore, the entire projected profile of the thin filament would appear approximately the same, regardless of the number of attached cross-bridges. On the other hand, in the rigor state Fig. 1 *b*, a larger portion of the myosin head is immobilized. With an orderly array of immobilized myosin heads attached to it, the thin filament should appear enlarged. Such an interpretation is consistent with the earlier suggestion by Matsuda and Podolsky (1984) that the flexibility in binding of attached cross-bridges is different between the relaxed and rigor states.

At the center of the backbone of the thick filament, both difference maps show an increase in density. In Fig. 1 *c* the total mass in the backbone area remains unchanged. This could mean that the thick filament is better ordered as ionic strength is lowered. In Fig. 1 *b*, however, there is a net loss of mass from the backbone. It was suggested that the S2 portion of myosin is probably an integral part of the backbone (Yu et al., 1985). This loss of mass suggests that there is an outward movement of S2 as the muscle goes into rigor.

In summary, we conclude that the differences between redistributions of mass after attachment of the cross-bridges when lowering ionic strength in relaxed fibers and when going into rigor very likely reflect different attachment configurations. Our axially projected two-dimensional difference maps suggest that the part of myosin head immobilized by attachment is smaller in the relaxed state than in rigor state. Furthermore, the attached cross-bridges in relaxed fibers move more freely around the thin filament than those in the rigor fibers.

Received for publication 28 May 1985.

REFERENCES

Brenner, B., M. Schoenberg, J. M. Chalovich, L. E. Greene, and E. Eisenberg. 1982. Evidence for cross-bridge attachment in relaxed muscle at low ionic strength. *Proc. Natl. Acad. Sci. USA.* 79:7288–7291.

Brenner, B., L. Yu, and R. J. Podolsky. 1984. X-ray diffraction evidence for cross-bridge formation in relaxed muscle fibers at various ionic strengths. *Biophys. J.* 46:299–306.

Matsuda, T., and R. J. Podolsky. 1984. X-ray evidence for two structural states of the actomyosin cross-bridge in muscle fibers. *Proc. Natl. Acad. Sci. USA.* 81:2364–2368.

Yu, L. C., A. C. Steven, G. R. S. Naylor, R. C. Gamble, and R. J. Podolsky. 1985. Distribution of mass in relaxed frog skeletal muscle and its redistribution upon activation. *Biophys. J.* 47:311–321.

CROSSBRIDGE AND BACKBONE STRUCTURE OF INVERTEBRATE THICK FILAMENTS

RHEA J. C. LEVINE, ROBERT W. KENSLER, AND PAT LEVITT
Department of Anatomy, The Medical College of Pennsylvania, Philadelphia, Pennsylvania 19129

We and others have previously shown that the cross-bridges of the filaments of the chelicerate arthropods (*Limulus*, tarantula, and scorpion) lie at a radius of 4 nm from the filament surface in a highly ordered four-stranded helical array with a repeat every 43.5 nm and an axial rise of 14.5 nm between cross-bridge levels (1–4).

Here we describe the effects of altering environmental conditions on the helical arrangement and radial extension of cross-bridges on *Limulus* thick filaments and present preliminary results of monoclonal antibody localization of paramyosin epitopes in myofibrils, on filaments and filament cores.

MATERIALS AND METHODS

Thick filaments were isolated in relaxing solution from unstimulated *Limulus* telson levator muscles, as previously described (1–3). While still in a thin film of liquid on the grid, the filaments were exposed to the solutions listed on Table I, to determine whether environmental conditions affect the cross-bridge arrangement and if such changes are reversible.

In separate experiments, *Limulus* myofibrils and native and myosin-

TABLE I
SUMMARY OF EFFECTS OF ENVIRONMENTAL CONDITIONS ON RADIAL POSITION OF CROSSBRIDGE CENTERS OF MASS AND FILAMENT DIAMETER

Conditions	Mean Radius of Crossbridge Mass*	Filament Diameter‡
	nm	*nm*
Relaxed	14.5 – 15.5	30
Rigor (−ATP)	18.2	36
EDTA (−Mg2+)	17.3	35
50% ethylene glycol (glycol)	17.6	35
0.2 MKCl	§	38
pH 8.0	§	40
pyrophosphate (pp)	16.5	33
Rigor and 1 mm Ca^{2+}	14.7	29
Rerelaxed from Rigor	14.5	29
Rerelaxed from EDTA	15.5	31
Rerelaxed from Glycol	15.7	31
Rerelaxed from pp	14.9	30

*Values were calculated from subsidiary maxima on LL3 or the radial position of primary maxima on LL1 of optical transforms.
‡Values were measured directly on electron micrographs.
§Extreme disorder and loss of helical periodicity made this value unobtainable.

stripped (by incubation with 0.4 M KCl) (5) thick filaments were incubated with monoclonal antibodies to different regions of paramyosin as determined by immunoblots of electrophoretically separated fragments of sequentially digested *Limulus* paramyosin (6). Myofibrils were incubated secondarily with fluorescein isothiocyanate (FITC) conjugated to rabbit antimouse antisera (Accurate Chemical Co., Westbury, NY). Native filaments and paramyosin cores were incubated with the primary antibody only, directly on carbon-coated grids. Controls were incubated with antibody previously absorbed vs. precipitated paramyosin.

Paired phase and fluorescence micrographs of myofibrils were taken on a Leitz Ortholux microscope (E. Leitz, Inc., Rockleigh, NJ) using epifluorescent illumination.

All filaments and cores were negatively stained, examined and photographed at in a Jeolco 100S electron microscope (JEOL, USA, Peabody, MA), at 80 KV using the anticontamination device (1). Optical transforms obtained from the electron micrograph negatives were analyzed as previously described (1–3).

RESULTS

Environmental Effects on Thick Filaments

Table I shows the effects of exposure of originally relaxed filaments to the experimental conditions and re-exposure to relaxing solution. Most experimental solutions (except for 1 mM Ca^{2+} in rigor buffer) induced cross-bridge movement away from the filaments' surfaces, with varying degrees of disordering of their helical periodicity (Fig. 1). Re-exposure to normal relaxing solution after incubation in rigor buffer, ethylene diamine tetracetic acid (EDTA), glycol, or pyrophosphate (PP) restored the radial position and helical arrangement of cross-bridges, and the filaments appeared similar to untreated ones and produced well-ordered optical transforms (Fig. 1).

Paramyosin Epitopes on Thick Filaments

Two monoclonal antibodies 11_1F_6 and 11_2E_3, directed toward different epitopes on the amino-terminal portion of *Limulus* paramyosin, stained different A-band regions in *Limulus* myofibrils (Fig. 2 *a*, *b*). Antibodies specific for epitopes closer to the carboxy-terminal of paramyosin did not stain A-bands. Individual antibody molecules of both 11_1F_6 and 11_2E_3 bound near the tips of native thick filaments and 11_2E_3 also bound to regions on either side of the bare zones (Fig. 2 *c*). Both antibodies bound in periodic fashion (about every 75 nm) to filament cores (Fig. 2 *d*).

DISCUSSION

Nucleotide presence (or absence) and the ionic and osmotic milieu affect the relaxed helical structure of *Limulus* thick filaments so that cross-bridge movement away from the shaft occurs in the absence of a thick-thin filament lattice. This effect is reversible, because cross-bridges return to their relaxed conformation after re-exposure to relaxing solution. These observations warrant further study. The calcium-mediated inhibition of the effect of rigor buffer may be due to the presence of calmodulin and light-chain kinase in the filament suspension, resulting in myosin phosphorylation (7). Our results suggest that cross-bridge behavior can be analyzed by examination of this isolated system.

Promising results have also been obtained using monoclonal antibodies to map paramyosin epitopes on *Limulus* thick filaments. Sites on paramyosin other than those near the amino terminal are inaccessible to antibody binding in native thick filaments (isolated and in situ), probably because they are covered by cortical myosin molecules. Because antibodies that do bind attach to few and relatively specific sites along native filaments, while they bind every 75 nm along myosin-stripped cores, only a few paramyosin epitopes are exposed on intact structures. Such antibody binding may localize less-tightly packed regions in the filaments and these sites may be involved in the molecular disaggregation that we have suggested as the mechanism responsible for the activation-induced shortening of *Limulus* thick filaments (8).

We thank Drs. J. Wray and J. Woodhead for discussion, Ms. H. King and R. Bingler for photographic, and K. Golden for secretarial help.

This work was supported in part by U. S. Public Health Service grants AM 30442 to R. W. Kensler; AM33302 and HL15835 by the Pennsylvania Muscle Institute to R. C. Levine; and NS19606 by the March of Dimes and Birth Defect Foundation grant 1-919 to P. Levitt.

Received for publication 30 April 1985.

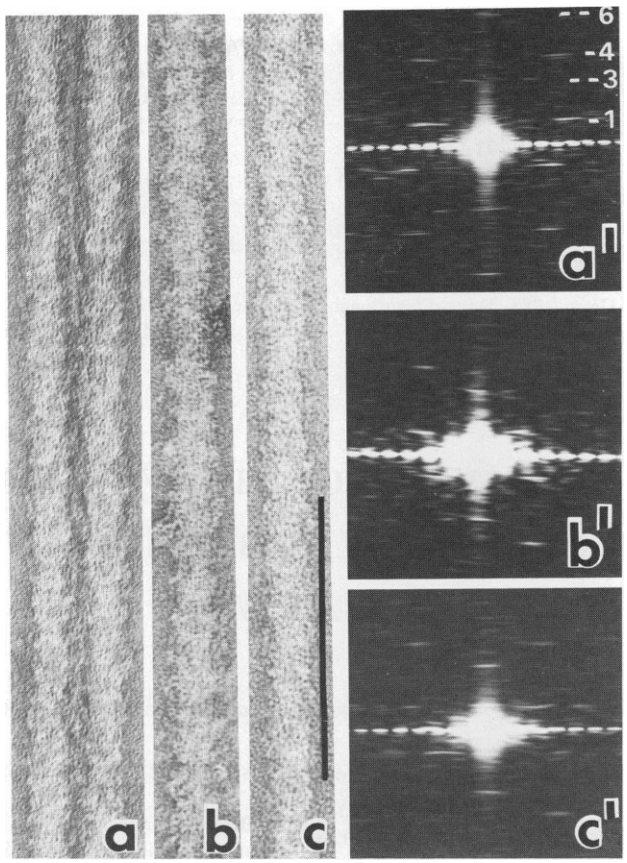

FIGURE 1 Electron micrographs of negatively stained thick filaments and optical transforms from them. (*a*) Relaxed filaments showing helical periodicity of the cross-bridge arrangement. (*b*) Filament after exposure to 50° glycol in relaxing solution shows radial extension of bridges and reduced order. (*c*) Filament re-relaxed after glycol exposure shows the return of cross-bridge order. Bar = 0.2 μm. *a'*, *b'*, and *c'* are optical transforms that show: *a'*, the original ordered structure; *b'*, the loss of information on the layer lines and narrowing of the pattern (increase in filament diameter); and *c'*, the return to an ordered structure. Layer lines are numbered on *a'*.

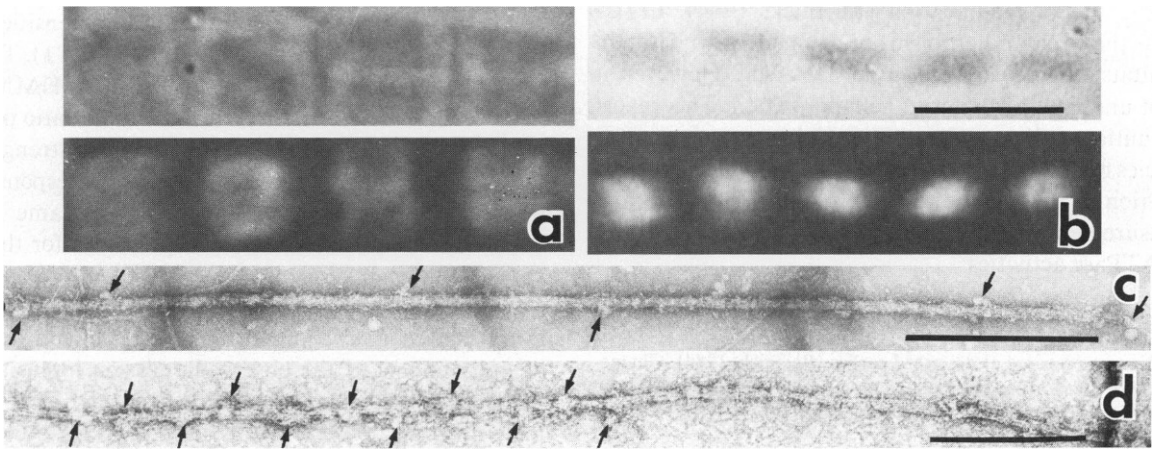

FIGURE 2 Monoclonal antibody binding to *Limulus* thick filaments. (*a*) Paired phase and fluorescence micrographs of 11_1F_6 staining laterally in the A-bands of *Limulus* myofibrils. This antibody binds only to the most amino-terminal fragment of paramyosin. (*b*) Paired and fluorescence micrographs of 11_2E_3 staining a central doublet in the A-bands of *Limulus* myofibrils. This antibody binds to a region further from the amino terminal of paramyosin. Bar = 10 μm. (*c*) 11_2E_3 binding along native *Limulus* thick filament. Arrows indicate sites of antibody binding. Bar = 0.5 μm. *d*. 11_2E_3 binding about every 75 nm along myosin-stripped thick filament core. Arrows indicate antibody. Bar = 0.2 μm.

REFERENCES

1. Kensler, R. W., and R. J. C. Levine. 1982. An electron microscopic and optical diffraction analysis of *Limulus* telson muscle thick filaments. *J. Cell Biol.* 92:443–451.
2. Levine, R. J. C., R. W. Kensler, M. C. Reedy, W. Hofmann, and H. A. King. 1983. Structure and paramyosin content of tarantula thick filaments. *J. Cell Biol.* 97:186–195.
3. Kensler, R. W., R. J. C. Levine, and M. Stewart. 1985. An electron microscopic and optical diffraction analysis of the structure of scorpion thick filaments. *J. Cell Biol.* In press.
4. Crowther, R. A., R. Padron, and R. Craig. 1985. Three-dimensional structure of tarantula thick filaments. *J. Mol. Biol.* In press.
5. Levine, R. J. C., R. W. Kensler, M. Stewart, and J. C. Haselgrove. 1982. The molecular organization of *Limulus* thick filaments. *In* Basic Biology of Muscles: A Comparative Approach. B. M. Twarog, R. J. C. Levine, and M. M. Dewey, editors. Raven Press, New York. 37–52.
6. Cowgill, R. W. 1975. Proteolysis of paramyosin from *Mercenaria mercenaria* and properties of its most stable segment. *Biochem. J.* 14:503–509.
7. Sellers, J. R. 1981. Phosphorylation-dependent regulation of *Limulus* myosin. *J. Biol. Chem.* 256:9274–9278.
8. Levine, R. J. C., and R. W. Kensler. 1985. Structure of short thick filaments from *Limulus* muscle. *J. Mol. Biol.* 182:347–352.

DIFFERENTIAL BEHAVIOR OF HEAVY MEROMYOSIN AND HEAVY MEROMYOSIN SUBFRAGMENT 1 TOWARD A MONOMERIC ACTIN DERIVATIVE

L. D. BURTNICK

Department of Chemistry, University of British Columbia, Vancouver V6T 1Y6, Canada

Actin and myosin in muscle act together to catalyse the hydrolysis of ATP and to couple the chemical energy released in this process to a mechanical event, contraction. In vitro, the Mg^{2+}-ATPase activities of myosin and its proteolytic fragments heavy meromyosin (HMM) and HMM subfragment-1 (S1) are stimulated in the presence of F-actin. Like myosin, both HMM (Trinick and Offer, 1979) and S1 (Ando and Scales, 1985), in the absence of ATP, bind tightly to and induce bundle formation by F-actin filaments.

G-actin can be reacted with fluorescein isothiocyanate (FITC) to give a product, FITC-actin, in which Lys-61 is the prime site of modification (Burtnick, 1984). FITC-actin has the circular dichroism spectrum of native G-actin and inhibits the nuclease activity of DNAse I. However, it does not undergo salt-induced polymerization. This report details initial studies on the ability of this nonpolymerizable species of actin to interact with HMM and S1 by direct observation of the emission properties of FITC-actin and by measurement of FITC-acto-HMM and FITC-acto-S1 Mg^{2+}-ATPase activities.

MATERIALS AND METHODS

FITC-actin was prepared as described earlier (Burtnick, 1984). Chymotryptic HMM and S1, prepared according to Weeds and Taylor (1975), were generous gifts of Dr. C. M. Kay and Dr. R. S. Hodges of the University of Alberta.

Acto-S1 and acto-HMM ATPase assays were performed by following either the inorganic phosphate release (Fiske and SubbaRow, 1925) or the proton release (Talbot and Hodges, 1981) tht accompanies ATP hydrolysis.

Fluorescence measurements were performed on a Perkin-Elmer (Norwalk, CT) MPF-44B spectrofluorimeter equipped with a thermostatted cell holder. Excitation was at 494 nm and emission intensities were measured at 517 nm. Excitation and emission bandwidths were both 4 nm.

Before fluorescence or ATPase studies, FITC-actin was dialyzed extensively against 2 mM Tris-HCl, 1 mM dithiothreitol, 0.2 mM ATP, 0.2 mM $CaCl_2$, pH 7.6 (henceforth called Buffer A) and clarified by centrifugation at 80,000 × *g* for 20 min. Concentrations of FITC-actin solutions were determined by amino acid analysis of duplicate samples that had been hydrolyzed for 20 h at 110°C in tubes that had been sealed under vacuum.

RESULTS

Addition of HMM to solutions of FITC-actin in solutions containing 100 mM KCl, 10 mM Tris-HCl, pH 8.0 resulted in quenching of the emission intensities of the samples to ~80% of their original levels (Fig. 1). The effect began to level off when the mole ratio of HMM:FITC-actin reached ~1.0; that is, when the mole ratio of myosin heads:actin units was ~2.0. When the ionic strength of the sample was reduced, the apparent lag in response of the fluorescence intensity to added HMM became less pronounced. As yet, a satisfactory explanation for this observation is lacking.

In contrast to the quenching of FITC-actin fluorescence that resulted in the presence of HMM, addition of S1 actually enhanced the observed emission intensities (Fig. 2). The enhancement reached 20–25% at S1 to FITC-actin mole ratios near seven. At higher mole ratios, the samples displayed a slight turbidity and the measured fluorescence intensities, as a result, began to decline. The single-headed S1 had an effect on the fluorescence of FITC-actin that required considerably more protein than did that of the double-headed HMM, suggesting a relatively weaker binding affinity of FITC-actin for S1 than for HMM.

BIOPHYS. J. © Biophysical Society · 0006–3495/86/01/138/02 $1.00
Volume 49 January 1986 138–139